Five-year climatology of tropical dry air intrusions as viewed by AIRS/Aqua

Sean P. F. Casey, A. E. Dessler and C. Schumacher
Department of Atmospheric Sciences
Texas A&M University

Many studies (Johnson et al. 1999; Redelsperger et al. 2002; Jensen and Del Genio 2006) have commented on the presence of mid-troposphere (400-600 hPa) dry air intrusions into normally moist areas of the warm pool region in the western Pacific, and their potential effects on the cumulus congestus cloud population. More recently, Zuidema et al. (2006) studied the effects of such intrusions over the eastern Pacific during the EPIC field campaign. However, no large-scale analysis of the occurrence and frequency of these intrusions in the tropics has been done. This is important to carry out, as a first step towards definitively determining the relation between dry air intrusions and cumulus congestus clouds.

To analyze these areas, water vapor mixing ratio measurements were taken from the Atmospheric Infrared Sounder (AIRS) instrument onboard the *Aqua* satellite. Five years of near-continuous data between September 2002 and August 2007 was used. As the presence of such dry air anomalies would be most prevalent over the warm tropical oceans, we limit our analysis to oceanic areas where the long-term (1968-1996) mean OLR, as calculated by NCEP, was less than 240 W/m^2.

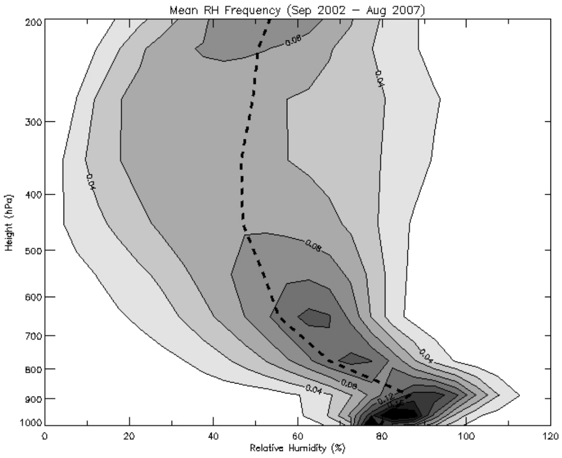

Figure 1: RH frequency of occurrence at each pressure level.

Figure 1 shows the frequency of occurrence at each pressure level for each level-2 relative humidity measurement with respect to liquid for T > 273 K and ice otherwise. In this and all following figures, observations were taken for ocean areas with a monthly mean OLR less than 240 W/m^2. The total values at each pressure level add up to 1. This figure shows that, though the air above the tropical oceans is normally very moist, there are moments of anomalously dry air.

Using relative humidity data over the eastern Pacific during the EPIC campaign, Zuidema et al. (2006) defined midlevel dry air intrusions as those instances where the relative humidity between 400 and 600 hPa was less than 40%. Using data from across the warm tropical oceans, however, it is apparent from Figure 1 that, while 40% is a low value for midlevel relative humidity, it is by no means anomalous. Therefore, we decided to define dry air intrusions for this study as those areas where relative humidity at these altitudes was less than 20%, a sufficiently low number when compared to the mean profile.

Figure 2 shows the total distribution of these midlevel dry air intrusions, graphed into 4° grid spacing. Adding all values on this graph together yields 100%. The thick solid line marks the boundary of areas where the long-term mean OLR is less than 240 W/m^2

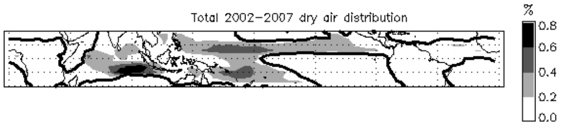

Figure 2: Total distribution of midlevel dry air intrusions.

for at least one calendar month. This shows an interesting prominence in mid-level dry air over the eastern Indian Ocean, with moderate values noted in the ITCZ and SPCZ.

Figure 3 separates out the total distribution by season. These graphs suggest that there are more intrusions into the northern Tropics in the boreal winter months and more into the southern Tropics in the austral winter. There's a clear maxima from June-November over the Indian Ocean. These months also happen to be when the Madden-Julian Oscillation (MJO) signal is weaker (Madden and Julian 1994); whether the two are causally related remains to be seen. The western Pacific signal also appears strongest in boreal winter [when the ITCZ signal is strongest (Garstang and Fitzjarrald 1999)], whereas that over the central/eastern Pacific is strongest in boreal summer and autumn. Finally, it's interesting to note the lack of a signal for midlevel dry air intrusions in the Atlantic Ocean, with the exception of boreal autumn.

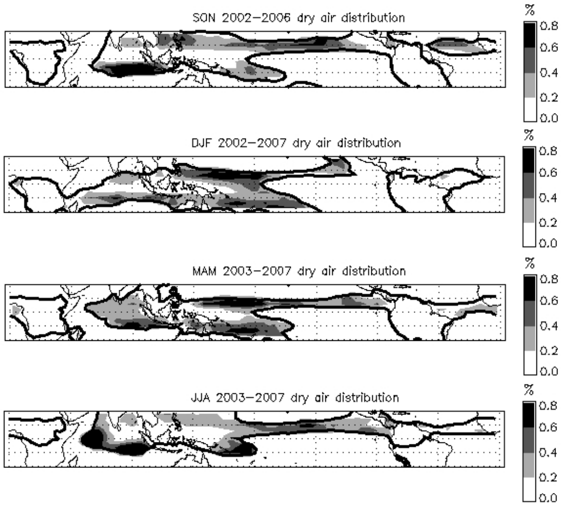

Figure 3: Same as in Figure 2, only separated by season.

Back trajectories outward to twenty days were calculated for each midlevel dry air region, using a trajectory program described in Bowman (1993). Along these back trajectories, we looked for the area for which these dry areas last condensed precipitation. To do this, temperature values were obtained for each past location using interpolation from NCEP data. Once obtained, the Goff-Gratch equation was used to estimate the saturation vapor pressure for this temperature. Assuming no changes in water vapor content since the time the air parcel last encountered convection, a calculated saturation water vapor content less than that measured initially by AIRS would suggest the parcel had condensed water and/or ice. This is defined as our time and location of origin for the dry air parcel.

Figure 4 shows the total distribution of these locations of dehydration. The most frequent source areas tended to be in the subtropics, with nodes of maxima over the northwestern Pacific and over Australia. Moderate sources of dry air were the Arabian Sea and the Eastern Pacific. Calculated source regions for some individual tracks extended well into the midlatitudes, with a few even

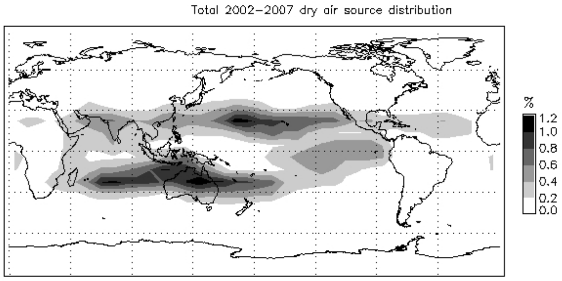

Figure 4: Total dry air source distribution.

originating poleward of 80°, though these appear to be outlier cases.

Figure 5 separates out the origin distribution by season. The long-term mean OLR boundaries from Figure 3 have been added to this figure as well. A few interesting features here. Tropics- and season-wide, it is apparent that the majority of dry air intrusions were last dehydrated in regions of higher mean OLR, signifying areas where less convection is present. The Arabian Sea appears to contribute the majority of its dry air intrusions in N.H. spring [mostly in May (not shown)], just preceding the onset of the Indian Monsoon. This is followed by lower counts in boreal summer, most likely resulting from the oceanic flow northward onto the Indian Subcontinent during the monsoon months. The Northern Pacific appears to be its most prominent in boreal winter, while the Eastern Pacific contributes moderate amounts of dry air intrusions during N.H. summer. These seem to correlate pretty well with the observations shown in Figure 5.

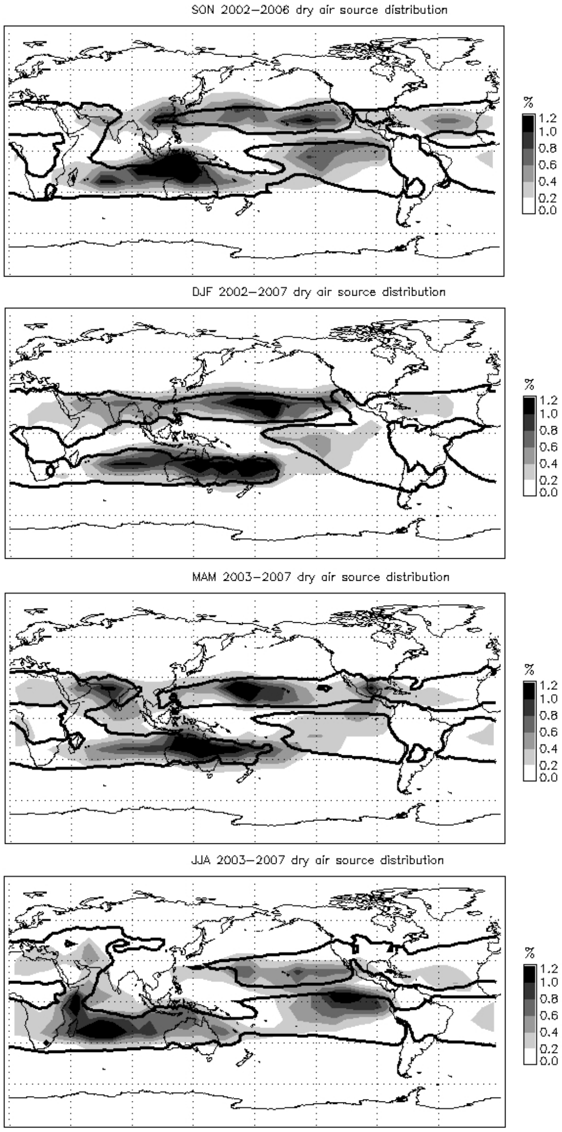

Figure 5: Same as in Figure 4, but separated by season.

Figure 6 shows the relative frequency of time from saturation to observation. The area under the curve integrates to one. It appears that the mean time since saturation is 3 days, with a exponential drop-off into longer time-periods. The sharp ending around 20 days should be disregarded, as the trajectories were only processed out this far.

Also on this figure is the seasonal separation. It is clear that the time from saturation to observation is about three days from September through to May, while the maximum time period from June-August is six days. Given that June-August is when

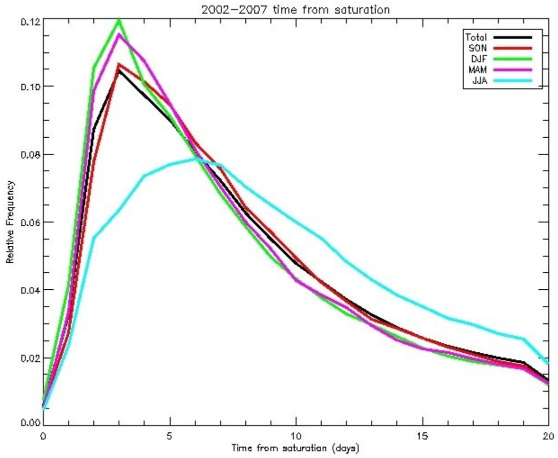

Figure 6: Relative frequency of time from saturation to observation.

Southern Hemisphere intrusions are most observed and that December-February is when N.H. intrusions mostly occur, this seems to suggest that either S.H. intrusions take longer to reach midlevels or that they last longer than N.H. intrusions.

References

Bowman, K. P (1993), Large-scale isentropic mixing properties of the Antarctic polar vortex from analyzed winds, *JGR-Atmos.*, *98*, D12, 23013-23027.

Garstang, M., and D. R. Fitzjarrald, Observations of Surface to Atmosphere Interactions in the Tropics. Oxford University Press, 1999.

Jensen, M. P., and A. D. Del Genio (2006), Factors limiting convective cloud-top height at the ARM Nauru Island climate research facility, *J. Climate*, *19*, 2105-2117.

Johnson, R. H., T. Rickenbach, S. A. Rutledge, P. Ciesielski, and W. Schubert (1999), Trimodal characteristics of tropical convection, *J. Climate*, *12*, 2397-2418.

Madden, R. A. and P. R. Julian (1994), Observations of the 40-50-Day Tropical Oscillation—A Review, *Mon. Wea. Rev.*, *122*, 814-837.

Redelsperger, J.-L., D. Parsons, and F. Guichard (2002), Recovery processes and factors limiting cloud-top height following the arrival of a dry intrusion observed during TOGA COARE, *J. Atmos. Sci.*, *59*, 2438-2457.

Zuidema, P., B. Mapes, J. Lin, C. Fairall, and G. Wick (2006), The interaction of clouds and dry air in the eastern tropical Pacific, *J. Climate*, *39*, 4531-4544.